Review

progress in Reaction Kinetics and Mechanism

Progress in Reaction Kinetics and Mechanism
Volume 49: 1–26

DOI: 10.1177/14686783241226858
journals.sagepub.com/home/prk
Sage

Understanding the rate-limiting step adsorption kinetics onto biomaterials for mechanism adsorption control

Sahmoune Mohamed Nasser[1], Moussa Abbas[2] and Mohamed Trari[3]

Abstract

Biomaterials are a class of porous materials that have been widely exploited over the past two decades. However, the implications of controlling adsorption by rate-limiting steps are still not adequately established. Identifying the rate-limiting step is a promising approach for the design of adsorption systems. In this review, we study in detail the rate-limiting step of the adsorption of dyes in aqueous media on biomaterials to rationalize the factors governing the rate-limiting step involved in the adsorption process using empirical kinetics and mass transfer models. This knowledge is then applied to identify the best fit of these models to study the rate-controlling step involved in the adsorption process, which is crucial for the design of the adsorption system. This review first studies the limiting step of adsorption of dyes in an aqueous medium on biomaterials. Kinetic modeling is used to better understand the rate control step involved in biosorption. Generally, the equations used are empirical models of kinetics and mass transfer and the biomaterials come from the following categories: agricultural and industrial waste, algae, fungi, bacteria, and plants. In most adsorption studies reported in this review, the pseudo second-order model was found to be best suited for fitting the kinetic data of dyes on biomaterials, indicating that chemisorption is the rate-limiting step that controls adsorption. Concerning the diffusion effects of mass transfer, intraparticle diffusion is among the most often used models to examine the rate-limiting step which is controlled by both film diffusion and intraparticle diffusion. The first takes place when the external transfer is

[1]Laboratory of Coatings, Materials and Environment, Department of Process Engineering, Faculty of Technology, University M'hamed Bougara of Boumerdes, Boumerdes, Algeria
[2]Laboratory of Applied Chemistry and Materials (LabCAM), University of M'hamed Bougara of Boumerdes, Boumerdes, Algeria
[3]Laboratory of Storage and Valorization of Renewable Energies, Faculty of Chemistry (USTHB), Algiers, Algeria

Corresponding author:
Moussa Abbas, Laboratory of Applied Chemistry and Materials (LabCAM), University of M'hamed Bougara of Boumerdes, Avenue de l'indépendance, Boumerdes 35000, Algeria.
Email: moussaiap@gmail.com

greater than the internal transfer while the opposite occurs in the case of porous diffusion. However, the majority of works do not study the real step of controlling the overall adsorption kinetics, namely, film diffusion or intraparticle diffusion.

Keywords
Adsorption, biomaterials, dyes, kinetic, rate-limiting step (RLS), modeling

Introduction

The elimination of heavy metals and dyes from aqueous industrial streams is of environmental interest due to their persistent nature in the aquatic environment. These pollutants bio accumulate in organic tissues, thus causing several metabolic dysfunctions. Globally, synthetic dyes are widely used in the textile, paper, printing, plastics, leather, food, and cosmetics industries. The elimination of heavy metals and dyes from industrial effluents is of environmental interest due to their persistent nature in the aquatic environment. These pollutants bioaccumulate in organic tissues, thus causing several metabolic dyes functions. Indeed, synthetic dyes are widely used in textile, paper, printing, plastic, leather, food, and cosmetics. An assortment of pollutants such as dyes, degradable organics, surfactants, heavy metals, and pH adjustment chemicals may be established in the textile wastewaters. In addition, colored effluents have a dramatic effect on the photosynthetic processes of the aquatic environment, causing low oxygen levels in the water and in severe cases, leading to asphyxiation of aquatic fauna and flora.[1] An assortment of pollutants such as dyes, degradable organic materials, surfactants, and heavy metals can be established in wastewater. Additionally, colored effluent has a detrimental effect on photosynthesis in aquatic environments, thus causing low oxygen levels in the water which can lead to asphyxiation of flora and fauna. Currently, dyes are the main source of pollution due to their uncontrolled release into water resources.[2] Many technologies have been applied to their removal such as photocatalysis, ultrasonic treatment, biodegradation, membrane separation, advanced oxidation processes (AOPs), coagulation/flocculation, and adsorption.[3–10] The latter remains attractive because of the high cost of elimination of organics using activated carbon (AC). Nevertheless, it is still high cost when using commercial carbons and the research is focused on the elaboration of inexpensive biosorbents and biomasses. The pore surface area of the adsorbent was determined by the N_2 adsorption-desorption and this has motivated the search for alternative adsorbents such biomaterials. The latter remains attractive due to the low cost of eliminating organic matter using activated carbon (AC). However, the use of commercial coals remains expensive and research focuses on the development of low cost biosorbents and biomasses. The pore surface area of the adsorbent was determined by N_2 adsorption-desorption, which motivated the search of alternative adsorbents such as biomaterials.[11] Over the last decade, some studies have been published on different aspects of dye adsorption.[12–16] Paï et al.[17] recently discussed the color removal performance of anionic and cationic dyes by nanocomposites while Kathiresan et al.[18] reviewed a number of biological, chemical, and physical methods for the dyes removal along with their effectiveness while Yagub et al.[19] demonstrated factors affecting the dyes adsorption. Zhou et al.[20] have oriented their research on hybrid adsorbents such as clays/zeolites and their composites, biosorbents, and industrial by-products. Kyzas et al.[21] gave a summary of how chitosan works for the removal of various dyes; Bhatia et al.[22] also reviewed biological methods employed to eliminate dyes from wastewater

and several research studies continue to emerge in the area of the dyes elimination using biomaterials.

Despite several available works on dye removal, no detailed kinetic studies have been dedicated to providing in-depth insights into the limiting step of dye adsorption. The accuracy obtained from adsorption processes depends on the modeling and interpretation of adsorption kinetics. Linear regression analysis was frequently used to access the quality of adsorption kinetic performance. Nonlinear regression has also been studied where the adsorption reactions take place according to a complex mechanism with the rate determination step (RLS). It is an important factor in influencing adsorption because it can play a role in the kinetics; therefore identifying RLS is essential for designing adsorption. Furthermore, it would be difficult to discuss adsorption mechanisms without knowledge of RLS, and many kinetic studies focus on RLS questions. This concept is important to be introduced to authors exploring the use of adsorbents for the removal of organic molecules in general and dyes in particular. The present work was designed in detail to comprehensively study the RLS that controls the adsorption process by biomaterials such as algae, fungi, bacteria, agricultural and industrial wastes, and plants. Therefore, RLS needs to be explained to authors exploring the use of adsorbents. This review will help the scientific community to strengthen the conceptual knowledge and prediction of RLS for adsorption design and modeling.

Rate-limiting step

One of the major aspects of any adsorption kinetic study is the investigation of RLS, that is, the kinetic that governs the global process[23] and this is difficult for any system. Prediction of RLS is of great importance in the design of any adsorption system,[24] a key information for the evolution of the biosorption. In principle, the rate constant of dye adsorption by a biomaterial can be determined from the set of simultaneous rate equations for the individual steps of the mechanism, one for each step. However, the analytical solution of these differential equations is not always easy. The assumption of a single RLS can greatly simplify the calculation of adsorption. Furthermore, the rate equation of the adsorption mechanism is usually in a simple mathematical form. Using a kinetic model, it is possible to identify RLS of adsorption of dye molecules.[25,26]

During adsorption, at the solid-liquid interface, a number of steps are involved in the transfer of coloring species from the bulk to the surface of the biomaterial[27] (Figure 1):

Transport of coloring molecules towards the periphery of the biomaterial

Diffusion of molecules through the liquid film surrounding the absorbing particles (film diffusion)

Dye molecules diffuse inside the intraparticle spaces and pores of the adsorbent (pore diffusion)

Fixation of these molecules on the sites of the adsorbent.

The limiting step corresponds to the overall speed of the process.[28] Previous studies have reported that the first and fourth stages are relatively rapid compared to the second and third stages.[29,30] Usually, film diffusion and pore diffusion are the important steps governing sorption rates. One of the two steps or their combination can therefore govern the process.[31] On the other hand, the pore diffusion controls the adsorption process for systems having high initial dye concentration, good mixing, large adsorbent particle size, and low affinity dye/biomaterial. Film diffusion is generally limiting in systems that have poor mixing, dilute dye concentration, low particle size, and high dye/biomaterial affinity.[32] In contrast, porous diffusion controls the adsorption process for systems with high initial dye concentration, good mixing, large adsorbent particle size, and low affinity dye/biomaterial.

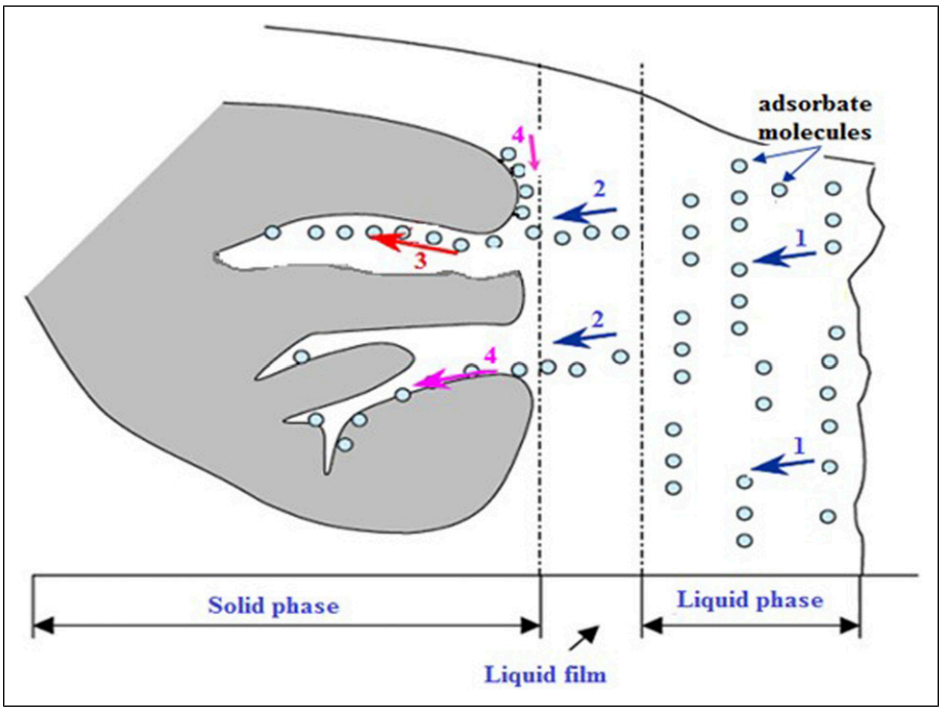

Figure 1. Adsorption of dye molecules from aqueous solution into the surface interior of the adsorbent.[27]

Kinetic modeling of adsorption

The main concern of environmentalists today is the presence of hazardous compounds in real effluents, resulting in dangers to many forms of life.[1–4] Over the past decades, the use of pharmaceuticals and dyes has increased significantly around the world. Given their implication on human health, their presence in the aquatic environment constitutes an emerging problem, which could have a long-term effect on ecological sustainability. Batch adsorption experiments represent an alternative for environmental protection. Adsorption efficiency is strongly dependent on pH and appears to be the reason why, in any adsorption study, optimizing the absorption rate as a function of pH is essential. Indeed, the pH conditions both the surface charge of the adsorbent as well as its structure. The remaining concentration of dyes was titrated by UV-visible spectrophotometry at the maximum wavelength (λ_{max}) and deduced by linear interpolation. The adsorbed quantity q_t (mg/g) and the percentage of dye removal R_t (%) by the biosorbent were calculated from the following equations

$$q_t = \frac{(C_0 - C_t) \cdot V}{m} \tag{1}$$

$$R_t = \frac{(C_0 - C_t) \cdot 100}{C_0} \tag{2}$$

C_o is the initial dye concentration, C_t is the concentration (mg/L) at time (t), V is the volume of solution (L), and m is the mass of biosorbent (g). Analysis of experimental data at different times

becomes feasible to calculate kinetic parameters and obtain information to design and model adsorption processes.[33] The adsorption kinetic is expressed by a graph presenting the variation of adsorbed dye by a biomaterial with contact time.[34] Kinetic modeling of adsorption is used to better understand the rate control step involved in the adsorption process.[35] Generally, the used equations are empirical kinetic models and mass transfer models.

Error function

Linear regression is one of the most pronounced and viable tools, frequently applied for the analysis of adsorption experimental data. The coefficient of determination (R^2) minimizes the distribution of errors between the experimental kinetic data and the predicted data. Nonlinear regression also leads to the minimization of error distribution; however, the operation is difficult in the absence of suitable algorithms. Due to the results obtained from the linearization of isothermal models and kinetic models, the determination coefficient R^2 is generally insufficient to predict the model which presents the best correlation. Thus, the application of error models, Root Mean Square Error (RMSE), the Sum of Error Squares (SSE), and Chi-Squares (X^2) test, equations (3), (4), and (5), respectively, are used as criteria for the quality of fitting. Due to the inherent bias resulting from linearization of the isotherm model and the kinetic model, for nonlinear regression, the coefficient (R^2) is insufficient to assess the goodness of fit. Thus, the application of the Root Mean Square Error (RMSE), the test equation of sum of square error (SSE), and chi-square (X^2), equations (3)–(5), respectively, are used as criteria for the quality of fitting

$$\mathrm{RMSE} = \sqrt{\frac{1}{\mathrm{N}-2} \cdot \sum_{1}^{\mathrm{N}} \left(\mathrm{q}_{\mathrm{e,\,exp}} - \mathrm{q}_{\mathrm{e,\,cal}}\right)^2} \tag{3}$$

$$\mathrm{SSE} = \frac{1}{\mathrm{N}} \sum\nolimits_{\mathrm{n}=1}^{\infty} \left(\mathrm{qe}_{\mathrm{cal}} - \mathrm{qe}_{\mathrm{exp}}\right)^2 \tag{4}$$

$$\mathrm{X}^2 = \sum\nolimits_{1}^{\mathrm{N}} \frac{\left(\mathrm{q}_{\mathrm{e,\,exp}} - \mathrm{q}_{\mathrm{e,\,cal}}\right)^2}{\mathrm{q}_{\mathrm{e,\,cal}}} \tag{5}$$

where $q_{e(exp)}$ (mg/g) is the experimental value of uptake, $q_{e(cal)}$ is the calculated value using a model (mg/g), and N is the number of observations in the experiment (the number of data points); the smaller RMSE value indicates the better curve fitting.[13]

Empirical kinetic models

Pseudo first-order kinetic model. The equation for pseudo first-order kinetics introduced initially by Lagergren[36] is generally used in the form modified by Ho and McKay

$$\mathrm{Ln}[q_e - q(t)] = \mathrm{Ln}\, q_e - k_1 . t \tag{6}$$

with $q(t)$ being the amount of adsorbed solute at time (t), q_e its value at equilibrium, and k_1 the pseudo first-order rate constant.

This equation may also be written in the following alternative way

$$\mathrm{q(t)} = \mathrm{q_e}\,[1 - \exp(-\,\mathrm{k_1}\,.\,\mathrm{t})] \tag{7}$$

If q_e is determined from the experiment, the fractional uptake, with respect to equilibrium, may be computed

$$\mathrm{F}(t) \sim \frac{\mathrm{q}(t)}{\mathrm{q_e}} \tag{8}$$

Then, one would have in the case of k_1

$$\mathrm{F(t)} = [1 - \exp(-\mathrm{k_1}.\mathrm{t})] \tag{9}$$

This model suggests a physisorption with diffusion as the rate-controlling step.[37]

Pseudo second-order kinetic model. The pseudo second-order kinetics is generally employed in the form proposed by Ho and McKay[38]

$$\frac{\mathrm{t}}{\mathrm{q_t}} = \frac{1}{\mathrm{K_2}.\mathrm{q_e^2}} + \frac{1}{\mathrm{q_e}} \cdot \mathrm{t} \tag{10}$$

in which k_2 is the pseudo second-order kinetic rate constant; this equation may be rewritten as

$$\mathrm{q(t)} = \mathrm{q}_e \,.\, \mathrm{k_2^*}.\mathrm{t} \,/\, \left(1 + \mathrm{k_2^*}.\mathrm{t}\right) \tag{11}$$

$$\text{with}\, \mathrm{k_2}^* = \mathrm{k_2}\,.\,\mathrm{q_e}^2 \tag{12}$$

$$\mathrm{F(t)} \sim \mathrm{k_2^*}.\,\mathrm{t} / \left(1 + \mathrm{k_2^*}.\mathrm{t}\right)$$

This model assumes that chemisorption is the rate-limiting step in adsorption. Previous studies have shown that the error structure of experimental data is generally changed when transforming adsorption kinetics into their linearized forms.[39] The pseudo second order presents four (4) linear forms. Therefore, there is the need to identify and clarify the usefulness of both linear and nonlinear regression analysis in various adsorption systems. It is against this backdrop that non-linearized regression analysis became inevitable, since it provides a mathematically rigorous method for determining adsorption parameters using original form of kinetic equations.

Elovich equation. The Elovich equation is expressed by the relation[40]

$$\frac{dq}{dt} = a_E e^{-\beta_E q} \tag{13}$$

Integration of the rate constant leads to the linear form

$$q_t = \frac{1}{\beta_E}\ln(a_E\beta_E) + \frac{1}{\beta_E}\ln t \tag{14}$$

where a_E (mg/g s) is the initial sorption rate, and β_E is (g/mg) related to the extent of surface coverage and activation energy for the chemisorption.

Mass transfer models

Intraparticle diffusion equation. The intraparticle diffusion equation is given by[41]

$$q_t = k_{id} t^{0.5} + C \tag{15}$$

k_{id} represents the rate constant (mg/g $min^{0.5}$), and the constant C (mg/g) gives an idea on the thickness of the boundary layer. When intraparticle diffusion is the limiting step, then the plot q_t versus $t^{0.5}$ passes by the origin; if not, RLS is affected by both the film diffusion and intraparticle diffusion.

Bangham equation. The Bangham equation is used to describe the diffusion of the pollutant into the pores of the adsorbent. In this model, dye molecules move from the surface to the interior sites of the particles by diffusion into pores; this model is the generalization of that of Weber and Morris[42,43] whose equation is expressed as follows[44]

$$\text{loglog}\left(\frac{C_0}{C_0 - q_t m}\right) = \log\left(\frac{k_0}{2.303V}\right) + \alpha \log t \tag{16}$$

where $\boldsymbol{C_o}$ is the initial dye concentration, $\boldsymbol{V}$ is the volume of the solution, $\boldsymbol{m}$ is the weight of the adsorbent, $\boldsymbol{q_t}$ is the amount of the adsorbent fixed at time t, and $\boldsymbol{\alpha}$ and $\boldsymbol{k_o}$ are constants. The plot **log [log {C_i/(C_i -q_t . m)}]**against **log (t)** gives a straight line if the sorption process involves pore diffusion.

In general, three steps are involved in the adsorption, namely, the extra-granular diffusion, intra-granular diffusion, and interaction of the adsorbate with the active sites of the adsorbent. Among these steps, the third is very fast and therefore is not the limiting step, and the overall adsorption process can be controlled by the first two steps; the Bangham equation is applied in this study to check whether the pore diffusion is the limiting step or not.

Boyd plot. The Boyd kinetic expression is[45]

$$F = 1 - \frac{6}{\pi^2}\exp(-Bt) \tag{17}$$

where $\boldsymbol{B}$ is a constant, and $\boldsymbol{F}$ is the fractional achievement of equilibrium at time $\boldsymbol{t}$, which is given by

$$F = \frac{q_t}{q_e} \tag{18}$$

Substituting the value of $\boldsymbol{F}$in equation (15) gives the following expression

$$Bt = -0.4977 - \ln(1 - F) \tag{19}$$

The $\boldsymbol{Bt}$ values at different contact times are calculated from equation (19), and intervals are plotted against time t. The line passing through the origin indicates adsorption governed by intra-article diffusion; otherwise, the process is controlled by the release of the film.

External mass transfer model. This model describes the evolution of the concentration of the solute C (mg/L) in the solution, as a function of the difference in the concentrations in the solution C and on the surface of the particles Cs (mg/l), according to the following equation[46]

$$\frac{dC}{dt} = \beta S(C - C_S) \tag{20}$$

β is the mass transfer coefficient (m s^{-1}), and $\boldsymbol{S}$ is the surface area of the adsorbent (m^2/g). The coefficients were determined after making some assumptions such as a surface concentration $\boldsymbol{C_s}$ negligible at initial (t = 0), a concentration in solution tending to the initial concentration C_o, and also negligible intraparticle diffusion; so the previous equation can be simplified to

$$\left[\frac{d(C/C_0)}{dt}\right]_{t\to 0} = -\beta S \tag{21}$$

Hence, at $t \to 0$, a plot of C/C_o gives a slope of $-\beta S$ from which β can be determined.

Kinetic studies in dyes adsorption on various kinds of biomaterials

Many biomaterials have been studied to remove dyes in aqueous environments. For the sake of understanding, biomaterials are subdivided into the following sections:

Algae

The word "algae" refers to a large and diverse group of eukaryotic organisms that contain chlorophyll and carry out oxygenic photosynthesis.[47] Numerous chemical groups are responsible for dye adsorption by algae, for example, amino, carboxyl, sulfate, and phosphate.[48] Algae used for the dye elimination include *Spirogyra sp,*[49] *Sargassum muticum,*[50,51] *Stoechospermum marginatum,*[52] *Spirulina platensis*,[53] *Turbinaria conoides,*[55] *Nostoc comminutum*,[56] *Cymopolia barbata*,[57] *Ulothrix sp*.,[58] and *Chlorella* sp.[59]

Khataee et al.[49] used *Spirogyra sp.* for the removal of three textile dyes, that is, Acid Orange 7, Basic Red 46, and Basic Blue 3 in batch processes. The pseudo second-order equation showed proper fitting with a high coefficient (R^2 >0.990) compared to the pseudo first-order model (R^2: 0.870−0.970). The R^2 values (0.92−0.98) for the intraparticle diffusion model are far from unity, suggesting that both the film diffusion and intra-particle diffusion are involved in the mass transfer limiting step. Authors stated that RLS is controlled by pore diffusion.

El Atouaniet al.[50] studied the batch sorption of methylene blue (MB) onto *Sargassum muticum* and the equilibrium was reached within 60 min. The kinetic data fitted well with the pseudo second-order model, indicating that RLS is involved in chemisorption. *Sargassum muticum* was modified with methanol for the MB removal from aqueous solution[51] showed that the equilibrium was achieved within the range (30–60 min). Adsorption kinetics obeys the pseudo second-order (PSO) model. The plotq_t versus $t^{0.5}$ represents a double linearity, with two well-distinguished stages: the first step is attributed to the boundary layer diffusion effect, whereas the second step is the intraparticle diffusion effect; RLS is the intraparticle diffusion. Daneshvar et al.[52] used macro alga *S. marginatum* to adsorb three acid dyes, namely, the Acid Blue 25, Acid Orange 7, and Acid Black 1, where the PSO model adequately models the data of their adsorption kinetics. The intraparticle diffusion model did not describe well the acid dyes adsorption onto *S. marginatum* as, evidenced by the low R^2 values, between 0.84 and 0.92. This poor conformity suggests that RLS is affected by both the film diffusion and intraparticle diffusion.

Dotto and Pinto[53] used *S. platensis* for the removal of FD&C Red N° 40 in batch experiments. From the intraparticle diffusion plot (q_t vs $t^{0.5}$), the adsorption follows two steps (Figure 2),

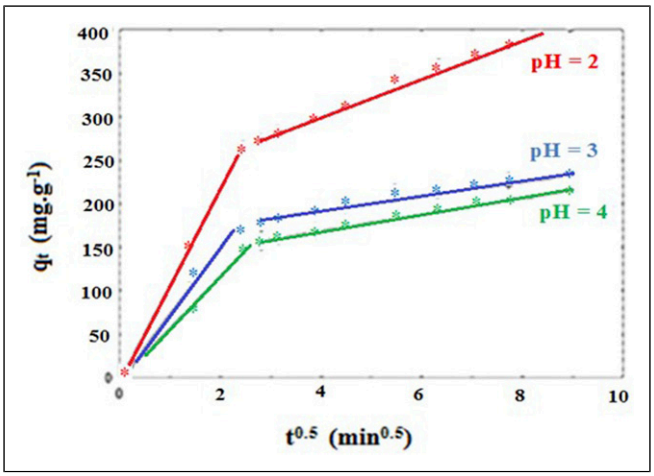

Figure 2. Intra-particle diffusion model plots for the sorption of FD&C red no. 40 by S. *platensis* at various pH.[53]

suggesting that both the film and intra-particle diffusion are rate-limiting steps of the adsorption of the dye FD&C Red onto *S. platensis.* The authors also used the Biot number (Bi*)* to confirm RLS; the film diffusion and intraparticle diffusion are the limiting steps when $1 < Bi < 100$.[54] The number Bi of FD&C Red no. 40 (1.65–10.33) is in the range (1–100) which indicates that RLS is controlled by external and internal mass transfer. The adsorption of Remazol brilliant blue (RBB) onto the biomass *T. conoides* has been investigated,[55] and the batch experiment showed that the equilibrium adsorption was reached within 90 min. The comparison of R^2 coefficients of the pseudo first order (PFO) is within the range (0.931−0.961) while the PSO model ($0.976 < R^2 < 0.998$) conceivably describes the mechanism and rate of uptake of RBB on *T. conoides*.

The removal of the Remazol Black 5 (RB) and RBB, hazardous dyes, from water by *N. comminutum* was investigated.[56] The adsorption was rapid within the first 50 min, and kinetic data of two dyes were well fitted with the PSO model (Table.1). On the other hand, the plot of the intra-particle diffusion showed three distinct regions, which indicate that RLS and both external mass transfer and intraparticle diffusion control the RBB adsorption.

Mullerova et al.[57] tested the modified macro algae *C. barbata* for Safranin O removal, where the time to reach the equilibrium did not exceed 90 min. The PSO model yielded the best fit with the coefficient R^2 of 0.996, while its value for the intra-particle diffusion model is low (0.836) with a nonlinear plot q_t versus $t^{0.5}$. This clearly indicates that both the intraparticle diffusion and film diffusion are involved in the Safranin O adsorption. The MB biosorption by *Ulothrix sp.* was studied[58] and the equilibrium was reached after 30 min of contact time where the PSO model exhibits kinetic analysis with R^2 coefficient close to unity (=0.998). On the contrary, the intraparticle diffusion model did not show a good fit with the kinetic data ($0.751 < R^2 < 0.976$), indicating that interstitial diffusion is not the only limiting step.

Chlorella sp. microalgal biochar could be used to remove MB and Congo red;[59] the dyes were adsorbed at the interface in a longer contact time (120 h) for MB and decreased considerably for Congo red (4 h) and the reason for this is a decrease in the number of sorption sites as well as the initial dye concentration (C_o). PFO models well to the kinetic analysis of the two dyes, where the concentration C_o increases from 10 to 60 mg/L, which consolidates the physisorption process with diffusion into the pores as the limiting step in the MB adsorption. On

Table 1. Kinetic studies of sorption of some dyes onto biomaterials.

Biomaterials	Dye	Teq (min)	Model	Rate-limiting step	Ref
Abelmoschus esculentus	Acridine orange	30	P.S.O	Film diffusion and intraparticle diffusion	104
Acetobacter *xylinum*	Direct blue 15	60	P.S.O	Chemisorption	79
Agaricus bisporus	Crystal violet	60	P.S.O	Film diffusion and intraparticle diffusion	66
	Brilliant green	40	P.S.O	Film diffusion and intraparticle diffusion	66
Aleppo pine-tree sawdust	Astrazon yellow	300	P.S.O	Film diffusion	106
	Basic Blue 3	300	P.S.O	Film diffusion	108
Almond shell	Eriochrome Black T	300	P.S.O	Film diffusion and pore diffusion	113
	Malachite green	300	P.S.O	Film diffusion and pore diffusion	113
Ananas comosus	Congo red	120	P.S.O	Film diffusion and pore diffusion	92
Areca nut husk	Brilliant green	40	P.S.O	Film diffusion	112
Aspergillus carbonarius	Congo red	180	P.S.O	Film diffusion and pore diffusion	65
Aspergillus fumigatus	Acid Violet 49	30	P.S.O	Film diffusion and intraparticle diffusion	63
Aspergillus wentii	Brilliant Blue G	180	P.S.O	Film diffusion and intraparticle diffusion	60
Azolla pinnata	Acid Blue 25	180	P.S.O	Film diffusion	85
Bacillus amyloliquefaciens	Acid Blue 225	90	P.S.O	Film diffusion and intraparticle diffusion	73
	Acid Blue 062	90	P.S.O	Film diffusion and intraparticle diffusion	73
Bacillus catenulatus	Basic Blue 3	10	P.S.O	Chemisorption	74
Bacillus fusiformis	Naphthalene	240	P.S.O	Chemisorption	71
Bacillus subtilis	Reactive Blue 4	240	P.F.O	Physisorption	78
Banana peels	Methylene blue	240	P.S.O	Film diffusion and intraparticle diffusion	101
	Orange G	240	P.S.O	Film diffusion and intraparticle diffusion	101
Black cumin	Methylene blue	30	P.S.O	Film diffusion	80
Breadnut peel	Methylene blue	60	P.S.O	Film diffusion and intraparticle diffusion	99
Burkholderia vietnamiensis	Crystal violet	60	P.F.O	Physisorption	76
Cabbage waste	Congo red	200	P.S.O	Chemisorption	88
Chlorella sp	Methylene blue	120 h	P.F.O	Pore diffusion	59
	Congo red	4 h	P.F.O	Film diffusion	59
Caesalpinia ferrea	Methylene blue	60	P.S.O	Film diffusion and intraparticle diffusion	86
Coffee husk waste	Methylene blue	200	P.S.O	Chemisorption	95
Cortaderia selloana	Methylene blue	240	P.S.O	Film diffusion andintraparticle diffusion	83

(continued)

Table 1. (continued)

Biomaterials	Dye	Teq (min)	Model	Rate-limiting step	Ref
Cucumber peels	Methylene blue	240	P.S.O	Film diffusion and intraparticle diffusion	101
	Orange G	240	P.S.O	Film diffusion and intraparticle diffusion	101
Cymopolia barbata	Safranin O	90	P.S.O	Film diffusion and intraparticle diffusion	57
Daedalea africana	Methylene blue	150	P.S.O	Film diffusion and intraparticle diffusion	68
Dietzia sp. PD1	Congo red	—	P.S.O	Chemisorption	70
	Indigo carmine		P.S.O	Chemisorption	70
Eichhornia crassipes	Congo red	90	P.S.O	Chemisorption	82
Enterolobium contortisiliquum	Methylene blue	180	Kinetic diffusion	Film diffusion	111
Ficus carica	Methylene blue	210	P.S.O	Film diffusion and pore diffusion	94
Funalia trogii	Congo red	60	P.S.O	Chemisorption	61
Haloxylon recurvum	Acid brown	50	P.S.O	Pore diffusion	87
Lawsonia inermis	Brilliant green	180	P.S.O	Film diffusion	93
Lentinus concinnus	Reactive Yellow 86	90	P.S.O	Chemisorption	62
Moringa seeds waste	Dispersed Red 60	45	P.S.O	Film diffusion and intraparticle diffusion	100
	Congo red	45	P.S.O	Film diffusion and intraparticle diffusion	100
Moringa oleifera	Reactive Red 120	30	P.S.O	Chemisorption	81
Nostoc comminutum	Remazol Black 5	50	P.S.O	Film diffusion and intraparticle diffusion	56
	Remazol brilliant blue	50	P.S.O	Film diffusion and intraparticle diffusion	56
Paenibacillus	Acid Blue 225	90	P.S.O	Film diffusion and intraparticle diffusion	72
macerans	Acid Blue 062	90	P.S.O	Film diffusion and intraparticle diffusion	72
Peanut husk	Indosol Yellow BG	30	P.S.O	Film diffusion and intraparticle diffusion	98
Pestalotiopsis sp	Remazol Brilliant Blue R	—	P.S.O	Film diffusion and intraparticle diffusion	69
Phragmites australis	Methylene blue	90	P.S.O	Chemisorption	91
Phragmites australis(modified)	Methylene blue	120	P.S.O	Chemisorption	91
Pine cone powder	Congo red	100	P.S.O	Film and pore diffusion	110

(continued)

Table 1. (continued)

Biomaterials	Dye	Teq (min)	Model	Rate-limiting step	Ref
Potato peels	Methylene blue	240	P.S.O	Film diffusion and intraparticle diffusion	101
	Orange G	240	P.S.O	Film diffusion and intraparticle diffusion	101
Prosopis juliflora	Victoria blue	40	P.S.O	Film diffusion and intraparticle diffusion	89
Raphia hookerie	Rhodamine B	50	P.S.O	Pore diffusion	109
Rhizophora mucronata	Crystal violet	60	P.S.O	Chemisorption	84
Rhizopus oryzae	Methylene blue	—	P.S.O	Film diffusion and intraparticle diffusion	67
Rhizopus arrhizus	Amaranth	240	P.S.O	Film diffusion and intraparticle diffusion	64
Rhizopus arrhizus	Fast Red A	240	P.S.O	Film diffusion and intraparticle diffusion	64
Rhizopus arrhizus	Congo red	240	P.S.O	Film diffusion and intraparticle diffusion	64
Rhizopus arrhizus	Tartrazine	240	P.S.O	Film diffusion and intraparticle diffusion	64
Rhizopus arrhizus	Metanil yellow	240	P.S.O	Film diffusion and intraparticle diffusion	64
Rhizopus arrhizus	Sunset Yellow FCF	240	P.S.O	Film diffusion and intraparticle diffusion	64
Rice husk	Diamine Green B	—	P.S.O	Film diffusion and intraparticle diffusion	102
	Acid Black 24	—	P.S.O	Film diffusion and intraparticle diffusion	102
	Congo red	—	P.S.O	Film diffusion and intraparticle diffusion	102
Sago waste	Alizarine Red-S	100	P.S.O	Film diffusion and intraparticle diffusion	96
Sargassum muticum	Methylene blue	60	P.S.O	Chemisorption	50
Sargassum Muticum (modified)	Methylene blue	30–60	P.S.O	Film diffusion and intraparticle diffusion	51
Soya bean	Acid Blue 25	180	P.S.O	Film diffusion	85
Sphagnum peat moss	Malachite green	90	P.S.O	Pore diffusion	90
Stoechospermum marginatum	Acid Blue 25	60	P.S.O	Film diffusion and intraparticle diffusion	52
	Acid Orange 7	60	P.S.O	Film diffusion and intraparticle diffusion	52
	Acid Black 1	60	P.S.O	Film diffusion and intraparticle diffusion	52
T. citrinoviride	Remazol Brilliant Blue R	—	P.S.O	Film diffusion and intraparticle diffusion	69
T. koningiopsis	Remazol Brilliant Blue R	—	P.S.O	Film diffusion and intraparticle diffusion-	69

(continued)

Table 1. (continued)

Biomaterials	Dye	Teq (min)	Model	Rate-limiting step	Ref
Sugar beet pulp	Reactive Red 2	20	P.S.O	Film diffusion and intraparticle diffusion	103
Turbinaria conoides	Remazol brilliant blue	90	P.S.O	Chemisorption	55
Ulothrix sp.	Methylene blue	30	P.S.O	Film diffusion and intraparticle diffusion	58

References: From 47 to 59, Biomaterials: Algae.
From 60 to 69, Biomaterials: Fungi.
From 70 to 79, Biomaterials: Bacteria.
From 80 to 94, Biomaterials: Plants.
From 95 to 113, Biomaterials: Agricultural and industrial wastes.

the contrary, the diffusion of the film turned out to be the determining step for the adsorption of Congo red.

Fungi

A large number of different fungal organisms are also known for the removal of different anionic and cationic dyes, including *Aspergillus wentii*,[60] *Funalia trogii*,[61] *Lentinus concinnus*,[62] *Aspergillus fumigates*,[63] *Rhizopus arrhizus*,[64] *Aspergillus carbonarius*,[65] *Penicillium glabrum*,[65] *Agaricus bisporus*,[66] *Rhizopus oryzae*,[67] *Daedalea Africana*,[68] *Phellinus adamantinus*,[68] *Turbinaria citrinoviride*,[69] *Turbinaria koningiopsis,* and *Pestalotiopsis* sp.[69]

Marine *A. wentii* was used for the elimination of Brilliant Blue G (BBG)[60] and the kinetic study showed that its adsorption increases over time and a complete saturation was reached after 180 min. The PSO model exhibited a better analysis for the kinetic data with a coefficient R^2 of 0.991, compared to 0.956 for PFO for the same biomass. However, the intra-particle diffusion plot revealed a multi-linearity pointing out that the film diffusion and intra-particle diffusion occurred simultaneously in the BBG adsorption. Bayramoglu and Arica[61] employed native and transformed Funalia *trogii* biomasses for the adsorption of Congo red in batch systems; the adsorption equilibrium was reached within 60 min for the two biomasses and both the PFO and PSO equations were used to describe the kinetic data. PSO delineated the absorption kinetics, indicating that chemisorption is RLS, which controls adsorption.

Bayramoglu and Arica[62] employed native and transformed Funalia *trogii* biomasses for the adsorption of Congo red in batch systems; the adsorption equilibrium was reached within 60 min for the two biomasses and both the PFO and PSO equations were used to describe the kinetic data. The Pseudo second order delineated the absorption kinetics, indicating that chemisorption is RLS, which controls adsorption.. Chaudhry et al.[63] used *Aspergillus fumigatu* as sorbent for the removal of Acid Violet 49. The kinetic was rapid and a saturation was reached after 30 min; PSO perfectly described the adsorption kinetic data; and the intraparticle diffusion plot presented a multi-linearity with three distinct phases. Therefore, both the film diffusion and intraparticle diffusion were identified to be RLS in the dye of Acid Violet 49. Salvi and Chattopadhyay[64] explored the dead fungal biomass of *R. arrhizus* for the elimination by adsorption of Amaranth, Fast Red A, Congo red, Tartrazine, Metanil yellow, and Sunset Yellow FCF in batch experiments. The different dyes were removed within the

first 100 min of contact time with the biosorbent and the saturation was reached after 4 h. The kinetic findings were best described by the PSO model. The intraparticle diffusion plot presented a multi-linearity indicating that two or more steps take place during the adsorption, which not only enclosed the processes of the liquid film diffusion and pore diffusion, but also the chemical adsorption with electrons exchanged between azo dyes and functional groups on the adsorbent surface.[64]

In the dyes adsorption, the point of zero charge (PZC) is an important parameter (Figure 3), especially when electrostatic forces are involved in the adsorption. Bouras et al.[65] examined the ability of *A. carbonarius* and *P. glabrum* to adsorb Congo red, an anionic and hazardous anionic dye. The kinetic study indicated that the sorption rates on both biosorbents follow the PSO, and the intraparticle diffusion is not RLS. Pandey *et* al.[66] reported the biosoprtion of Crystal Violet (CV) and Brilliant green (BG) onto *A. bisporus* in batch mode, and the equilibrium times were found to be 60 and 40 min, respectively; the authors described the PSO kinetics for the biosorption of both dyes and the adsorption was affected by the boundary layer diffusion and intraparticle diffusion. Dey et al.[67] studied the MB biosorption by live cells of *R. oryzae* in batch system and evaluated the kinetic study by applying the PSO and intraparticle diffusion models. The former perfectly fits the sorption data with high correlation coefficient ($R^2 = 0.999$). The *C*-values of the intra-particle diffusion model provide information on the thickness of the boundary layer, and the intercept of the intraparticle diffusion plot indicates a higher effect. The *C*-values of intra-particle diffusion model were higher than zero (1.35–9.47), suggesting that the mechanism of MB adsorption onto *Rhizopu soryzae* is not controlled by intraparticle diffusion. Therefore, both the film and pore diffusion are involved in the mass transfer controlling the MB adsorption onto *R. oryzae* biomass. Sintakindi and Ankamwar[68] carry out batch experiments to explore the kinetics of MB adsorption on *Daedalea africana* and *Phellinus adamantine*. The equilibrium time was reached between 150 and 180 min for *D. africana* and *P. adamantine,* while the kinetic follows the PSO model.

The intraparticle diffusion plots did not show straight lines, indicating that it is not the only rate-limiting step. Fungal strains of *T. citrinoviride*, *T. koningiopsis,* and *Pestalotiopsis* sp have been successfully tested for the adsorption of Remazol Brilliant Blue R,[69] and the fungal strains obey the

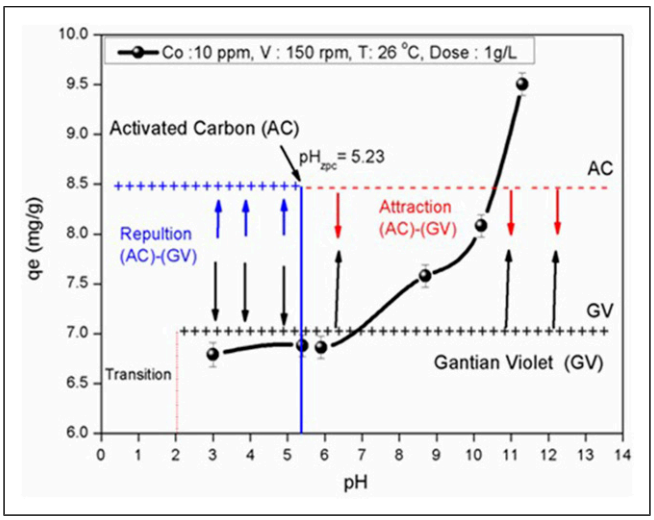

Figure 3. Effect of pH and isoelectric pH_{PZC} on crystal violet adsorption on activated carbon.[15]

PSO model. The *C*-value of intraparticle diffusion model was found in the range (0.063–0.326) for coefficients R^2 between 0.80 and 0.94. This points out that the pore diffusion is not RLS and the film diffusion may be concerned in the mass transfer mechanism.

Bacteria

Many authors worked with bacteria biomasses for the removal of dyes; these include *Dietzia sp.* PD1,[70] *Bacillus fusiformis*,[71] *Paenibacillus macerans*,[72] *Bacillus amylolique faciens*,[73] *Bacillus catenulatus*,[74] *Pseudomonas aeruginosa*,[75] *Burkholderia vietnamiensis*,[76] *Bacillus subtilis,*[78] and *Acetobacter xylinum*.[79]

Saha et al.[70] used *Dietzia sp.* PD1 for the removal of CR and Indigo carmine in batch experiments. The coefficients R^2 corresponding to the PSO model (0.997 and 0.993) were high compared to the PFO model (0.925 and 0.913) for both dyes, respectively, suggesting that chemisorption is RLS that governs the adsorption. Lin et al.[71] have also found that PSO perfectly described the adsorption kinetic of naphthalene onto immobilized Bacillus fusiformis. Living biomass, namely, *P. macerans* has been employed to remove Acid Blue 225 (AB225) and Acid Blue 062 (AB062)[72] and the data match well to the PSO model. The intraparticle diffusion model was applied to establish RLS of the adsorption of both dyes. The plots did not pass by the origin and this indicates that the intraparticle diffusion was not the solely rate-limiting step. Both anionic dyes AB225 and AB062 are also adsorbed onto *Bacillus amylolique faciens* at pH ~ 1[73] with an equilibrium time of 90 min. PSO provided the best determination coefficients for the adsorption of AB225 and AB062 by *Bacillus amylolique faciens* for all temperatures; RLS is complex, involving both the boundary layer and intraparticle diffusion.

Bacillus catenulatus strain JB-022 isolated from soil and polluted pond was explored for the Basic Blue 3 (BB3) removal.[74] A batch of experiments were performed. The BB3 adsorption was rapid and more than 80%; BB3 3 adsorption was achieved within 5 min , and the time required for attainment of the equilibrium did not exceed 10 min. The sorption kinetic of Basic Blue 3 follows well the PSO model.

Saravanan et al.[75] examined the potential of bacterium *P. aeruginosa* for Procion blue 2G removal. Elovich's model proved to be the best suited and corresponds to a chemisorption process. The low coefficient R^2 (=0.84) of intraparticle diffusion indicates that RLS is controlled by both surface and pore diffusion. The rate constant of intraparticle diffusion and effective diffusion coefficient calculated from the Boyd plot were, respectively, 1.133 mg/gmin$^{0.5}$ and 4.13 10^{-14} m^2/s for an initial dye concentration C_o of 100 mg/L. Zhou et al.[76] used *B. vietnamiensis* C09 V for the removal of Crystal violet and Cu (II). The Crystal violet removal fitted well to the PFO model, with a physisorption process, involving weak Van der Waals attraction between an adsorbate and adsorbent surface[77] with an enthalpy less than 10 kJ mol^{-1}. Similar findings were published by Binupriya et al.[78] for the biosorption of Reactive Blue 4 by free and immobilized *Bacillus subtilis*. The kinetics of Direct Blue 15 removal elimination using Acetobacter *Xylinum* has been investigated in batch configuration.[79] The equilibrium time occurred within 1 h at 45°C and was significantly dependent on the temperature. The PSO model gave a coefficient R^2 of 0.999 compared to 0.835 for PFO at 60°C.

Plants

In the open literature, some plants have been used for removal of dyes including Black cumin,[80] *Moringa oleifera*,[81] *Eichhornia crassipes*,[82] *Cortaderia selloana*,[83] *Rhizophora mucronata*,[84]

Azolla pinnata,[85] Soya Bean,[85] *Caesalpinia ferrea*,[86] *Haloxylon recurvum*,[87] Cabbage,[88] *Prosopis juliflora*,[89] Sphagnum peat moss[90,] *Phragmites australis*,[91] *Ananas comosus*,[92] *Lawsonia inermis,*[93] and *Ficus carica*.[94]

Siddiqui et al.[80] employed black cumin for the MB sorption and the effect of contact time showed a rapid kinetic with a complete saturation within 30 min. The kinetic experiment was described by the PSO model, where the plot q_t versus the square root of the contact time ($t^{0.5}$) does not pass by the origin. Therefore, the intraparticle diffusion is not RLS, and a boundary layer control may be involved in the biosorption. The Boyd equation was employed to prognosticate the slow step involved in the adsorption; the plots are linear but do not pass through the origin, thus confirming that the film diffusion is RLS. The adsorption of Reactive Red 120 on *M. oleifera* seed follows the Logistic and PSO model.[81] The time to reach equilibrium did not exceed 30 min for an initial dye concentration in the range (10–100 mg/L), adsorbent dose 0.5 g/L, and pH 1. Wanyonyi et al.[82] studied the elimination of CR by biosorption using the roots of *E. crassipes*. The sorption equilibrium reached 96% removal within 90 min. Kinetic data fit the PSO model well. The potential of *C. selloana* flower spikes as adsorbent for the MB removal was also reported.[83] The PSO model showed the data analysis ($R^2 = 0.997$), followed by PFO and Elovich equations. The intraparticle diffusion model did not fit suitably the kinetic data ($R^2 = 0.822$), indicating that the diffusion mechanism did not play the predominant role in the command of kinetics. *R. mucronata* bark was used for the CV elimination[84] and an optimum removal of 99.8% was reached within 60 min. The PSO model exhibited a better analysis for the kinetic data ($R^2 = 0.9998$) compared to 0.9768 for PFO. Therefore, RLS is a chemical reaction between the dye CV and binding sites. In addition, the non-zero intercepts of the intraparticle diffusion plots demonstrate that the intra-particle diffusion in the adsorption is not RLS for the adsorption of CV and BG dyes on fungal biomass.

Kooh et al.[85] tested *Azollapinnata* and soya bean wastes in the removal of Acid Blue 25 (AB25). The equilibrium was reached within 3 h for both adsorbents, and the data follow the PSO model. Weber and Morris plots do not pass by the origin, suggesting the non-validity of the intraparticle diffusion in the AB 25 adsorption and is not the only RLS. The authors analyzed the kinetic data also by using the Boyd model which displays linear profiles and does not pass by the origin, and this means that the film diffusion is RLS in the process. The MB removal by *C. ferrea* fruits was also explored,[86] and the kinetic study showed that the PSO model is appropriate with a good coefficient R^2 (=0.9828) compared to R^2 of 0.9766 and 0.9361 for the Elovich and PFO models, respectively. The intraparticle diffusion plot presents a multi-linearity with three distinct stages, where the adsorption was controlled by the boundary diffusion at the earlier stage followed by the pore diffusion. Hassan et al.[87] used *H. recurvum* plant for the removal of Acid brown and an optimal contact time for Acid brown of 50 min was determined; the adsorption obeys a PSO model and RLS is controlled by the pore diffusion. Wekoye et al.[88] examined cabbage waste powder for the CR removal in batch mode. The PSO and Elovich models supported the adsorption results while Kumar and Tamilarasan[89] reported the Victoria B uptake on modified *P. juliflora* in batch experiments with an equilibrium time of 40 min. The PSO model proved to be the most suitable model, and RLS is governed by the boundary layer diffusion and intraparticle diffusion. Hemmati et al.[90] investigated the kinetic of Malachite green (MG) onto Sphagnum peat. The equilibrium time was attained after 90 min with PSO as the best fitting ($R^2 > 0.9994$) compared to R^2 (0.9656−0.9711) for the PFO model. The plot q_t versus $t^{0.5}$ presents a multi-linearity with two distinct phases. With the constant k_{id1} (=7.7901 mg/g $min^{0.5}$, MG = 20 mg/L) as the diffusion rate constant of the exterior surface of the particle (film diffusion) and k_{id2} (=0.0393 mg/g $min^{0.5}$, MG = 20 mg/L) as the diffusion rate constant of the internal surface of the particles (intraparticle diffusion). RLS is controlled by the slowest step (intraparticle diffusion) in this case ($k_{id2} < k_{id1}$).

Kankılıçet al.[91] examined raw and modified *P. australis* as biosorbents for the MB upotake where the equilibrium time is between 90 and 120 min, respectively, and the MB adsorption follows the PSO model. Chan et al.[92] performed a series of batch experiments for the removal BB3 and CR by *A. comosus* plant stem. Practically 60–70% of the adsorption capacity was reached during the first 15 min of contact for both dyes and adsorption equilibrium was established over a longer period (120 min). The adsorption is best represented by the PSO kinetic model. For the intraparticle diffusion, the equation is not linear and does not by the origin for both dyes ($0.77 < R^2 < 0.94$), indicating that the adsorption of both dyes is rather complex, composed simultaneously of the boundary layer and intraparticle diffusions. The kinetic data fit the external mass transfer model well, and the film diffusion is the true RLS.

Modified *Law Sonia inermis* was used to eliminate the Brilliant green, a hazardous dye;[93] the uptake equilibrium was achieved within 3 h and the PSO model showed a better modeling of the adsorption kinetic. The intraparticle diffusion plots disclosed that the *C*-values increase from 2.4 to 6 mg/g with increasing the concentrations C_o from 25 to 100 mg/L. Raising the dye concentration C_o favors the boundary layer diffusion, thus implying that the film diffusion is the rate-controlling step.

Gupta et al.[94] endeavored to understand the mechanism of MB uptake by the modified *Ficuscarica*. Batch experiments were carried out, and the equilibrium time for the MB elimination was 210 min. The comparison of correlation coefficients of PFO ($R^2 = 0.953$), PSO ($R^2 = 0.998$), and intraparticle diffusion ($R^2 = 0.956$) kinetic models indicate that PSO best represents the mechanism and rate of the MB uptake. On the other hand, the film diffusion and pore diffusion are involved in the mass transfer controlling of MB molecules onto *Ficuscarica* plant.

Agricultural and industrial wastes

Agricultural and industrial wastes have been practiced as adsorbents for the dyes adsorption from water. The most commonly used adsorbents include coffee husk waste,[95] sago waste,[96] corn silk,[97] peanut husk,[98] breadnut peel,[99] *Moringa* seeds waste,[100] banana peels,[101] cucumber peels,[101] potato peels,[101] rice husk,[102] sugar beet pulp,[103] *Abelmoschus esculentus*,[104] palm-date stones,[105] Aleppo pine-tree sawdust,[106,108] *Raphia hookerie*,[109] pine cone powder,[110] *Enterolobium contortisiliquum,*[111] areca nut husk,[112] and almond shell.[113]

Tran et al.[95] investigated the batch experiment of the MB sorption onto the coffee husk waste and found that the equilibrium time increases with augmenting the MB concentration C_o. Optimal times were found to be 30, 120, 300, and 420 min for C_o-concentrations of 200, 300, 400, and 500 mg/L, respectively. PSO describes better the kinetic data based on the coefficient R^2 (=0.999) against the PFO model (0.911−0.985). The authors also found that the adsorption rate decreases with increasing C_o. Sago waste, a by-product obtained during the production of starch from tapioca was successfully tested to adsorb Alizarine Red-S;[96] the percentage removal increases with increasing the contact time and the best performance was observed within 100 min. The PSO model presents a high coefficient R^2 (=0.9983) compared to 0.9509 and 0.9558 for the PFO and intraparticle diffusion model, respectively. The coefficient R^2 (<1) means that intraparticle diffusion is not the only rate-limiting step, but consisting simultaneously of the boundary layer and intraparticle diffusions.

The adsorption potential of corn silk was explored for the removal of RB19 and RR218.[97] The kinetic data were well fitted by the PSO model; the greater R^2 values (∼1) confirm that the Bangham model is compatible with the kinetic data, suggesting that RLS is the pore diffusion. The potential of the adsorbent peanut husk to adsorb Indosol Yellow BG from water was described elsewhere.[98] The elimination is rapid (∼30 min) for a concentration C_o in the range (10–200 mg/L) with an adsorbent dose of 2 g/L. The PSO kinetic model assumed the best fit for the kinetic experiments, while the

intraparticle diffusion model provided a poor fit (R^2 = 0.413). This means that RLS is distributed between the film diffusion and intraparticle diffusion. The MB removal by breadnut peel was examined,[99] and the equilibrium was reached within 60 min; RLS is affected by both the boundary layer diffusion and intraparticle diffusion, and the adsorption kinetic followed the PSO model.

The adsorption capacity of *Moringa* seeds waste was used for the adsorption of Dispersed Red 60 (DR60) and CR from waters.[100] As expected, the percentage removal increases with increasing the contact time; the equilibrium was established within 45 min for both dyes, and the PSO model provided the best correspondence for their adsorption. The smaller R^2 values (0.5084–0.6843) confirm that the intraparticle diffusion model is inadequate to fit the kinetic data, and RLS is dispersed between the film diffusion and intraparticle diffusion.

Banana, cucumber, and potato peels were assessed as adsorbents to extract MB and Orange G from water.[101] The PSO model revealed a better agreement for both dyes, evidenced by the kinetic study. The high C values of the intra-particle diffusion model (7.09–78.65) prove the contributions of the film and intraparticle diffusion steps in the biosorption. The ability of rice husk to eliminate the anionic dyes, namely, Diamine Green B, Acid Black 24, and CR by adsorption was also studied,[102] and the kinetic data of the three dyes were modeled by the PSO model. The intra-particle diffusion linear plots showed three slopes which means that the intraparticle diffusion is not the only RLS.

Sugar beet pulp was modified by NH_4Br to prepare a novel sugar beet pulp adsorbent named SMSBP[103] and its adsorption capability for Reactive Red 2 was investigated; it exhibits a rapid kinetic with saturation reached beyond 20 min. The high R^2 values (0.996−0.999) appeared that the fixation of Reactive red 2 on the SMSBP follows rather the PSO equation, compared to PFO (R2: 0.892−0.924) with a limiting step dominated by the intraparticle diffusion.

Biosorption of Acridine orange by *Abelmoschuses culentus* was also studied,[104] and the analysis of kinetic data gave the values of R^2, HYBRD, RMSE, MPSD, ARE, APE, and chi-square χ^2. They are equal to (PFO: 0.8847, 265.4035, 22.6253, 8.8192, 12.5824, and 69.9021, 890.0836), (Elovich: 0.8387, 2.0464, 1.8620, 0.0825, 0.9543, 5.3017, and 1.9992), (Bangham: 0.9031, 0.6609 0.9981 0.0293, 0.4647, 2.5815, and 0.6289), (Modified-Freundlich: 0.8096,2.8477, 2.2643, 0.1062, 1.1056, 6.1420, and 2.8434), and (PSO: 0.9983, 1.2144 1.3206, 0.0561, 0.6234, 3.4635, and 1.1121). The greater R^2 (0.9983), smaller values of HYBRD (1.2144), smaller RMSE (1.3206), smaller MPSD (0.0561), smaller ARE (0.6234), smaller APE (3.4635), and smaller chi-square χ^2 (1.1121) indicated more suitability of PSO than the PFO, Elovich, Bangham, and modified-Freundlich models. The linear plot of intra-particle diffusion revealed two slopes, indicating that RLS is mainly controlled by external and internal mass transfer.

The biosorption of Basic Violet 3 and Basic Red 2 onto palm-date stones has been examined using the batch mode process.[105] The PSO equation presents a well kinetic analysis for both dyes with a high coefficient R^2 (>0.968). Regarding *the* high C values of the intra-particle diffusion model (35.68-51.00, > 0), this reveals that diffusion in the film and intraparticle diffusion contribute to the rate-limiting stage.. The pore diffusion is not the unique RLS, and the external mass transfer also controls the adsorption process in the first period.

Sahmoune and Ouazene[106] used the Aleppo pine-tree sawdust (APTS) for the Astrazon yellow uptake; APTS has been exploited to adsorb hazardous dyes due to its porous structure (Figure 4). The intra-particle diffusion plot presents two slopes, showing that both the film and pore diffusions are important in determining the global adsorption rate. The authors stated that the rate-limiting step was primarily film diffusion, similar to those describing the adsorption of tartrazine by sawdust.[107] APTS was also employed to adsorb Basic Blue 3 from water.[108] The kinetic data showed that the PSO model gave a correlation coefficient R^2 of 1 for a concentration C_o of 30 mg/L, compared to

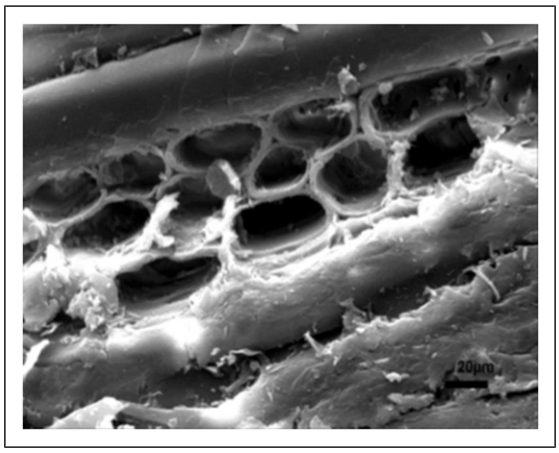

Figure 4. Scanning electron microscope image of Aleppo pine tree sawdust.[106]

0.9017 for the PFO equation. The Weber–Morris plot exhibits also two lines with constants (k_{id1} = 1.6421 and k_{id2} = 0.3573 (mg/g $min^{0.5}$) for Basic Blue (C_o = 100 mg/L). K_{id1} and k_{id2} are, respectively, the diffusion rate constants of the exterior and interior surfaces of the particle. k_{id2} is less than k_{id1} and this indicates that the slowest step is intraparticle diffusion, that is, the limiting step.

Inyinbor et al.[109] obtained similar results in the adsorption of Rhodamine B (Rh B), which is a calcitrant and stable dye, onto *Raphiahookerie*fruit epicarp. The PSO model better fits the adsorption kinetics. Rh B is a cationic dye soluble in water and belongs to the anthraquinone family; its mesomeric effect makes it difficult to eliminate by chemical and/or biological methods. The authors used the Bangham model, and the intraparticle diffusion model allows interpreting the slow step that could occur in the current adsorption system; however, the results revealed that the kinetic data do not fit well with the Bangham model. Therefore, the diffusion of Rh B molecules into pores of *R. hookerie* was not the only RLS; it also depends on the boundary layer diffusion and intraparticle diffusion plot is composed by two linear portions with the constants k_{id1} (=10.28) and k_{id2} (=3.73 mg/g $min^{0.5}$)for Rh B concentration of 100 mg/L. The constant k_{id1} is higher than k_{id2}, and this signifies that the uptake of Rhodamine B onto *R. hookerie* is mainly controlled by the pore diffusion

Dawood and Sen[110] examined the adsorption of CR by pine cone powder and the equilibrium time is 100 min and the kinetic data follows a PSO model. The intraparticle diffusion plot exhibits two distinct stages viz. film diffusion followed by a pore diffusion meaning that the CR molecules are transported to the external surface of the pine cone particles through the film diffusion; after wards the molecules are moved in pine cone particles by the intra-particle diffusion through the pores with a diffusion coefficient of 3.63×10^{-9} cm^2/s for an initial CR concentration of 50 mg/L.

Lima et al.[111] reported the kinetic of the MB biosorption onto *E. contortisiliquum*. Equilibrium time of 180 min was reached for a MB concentration in the range (10–40 mg/L), and the limiting step is governed by both the film diffusion and intraparticle diffusion. The Biot number (Bi) was used to investigate the real rate-controlling step involved in the overall adsorption system, that is, the film diffusion or intraparticle diffusion. The Bi values are in the range (0.04–0.1) for an initial MB concentration (10–50 mg/L; a low Bi value (<1) which indicates that RLS is controlled by the film diffusion. Baidya and Kumar reported the application of areca nut husk for the elimination of Brilliant green, a hazardous dye from water;[112] an equilibrium time of 120 min was determined. Their kinetic data were fitted by the PSO model with a high coefficient R^2 of 0.999; these authors

used the intraparticle model and Boyd plot to verify the RLS, and a nonlinearity is observed in the intraparticle diffusion plot. This implies that two processes (film and pore diffusion) limit the global adsorption rate, and the real RLS was analyzed by the Boyd plot which showed a linear behavior but does not pass by the origin, confirming that the external mass transfer is the slowest step. Arfi et al.[113] employed almond shell to eliminate Eriochrome Black T (EBT) and Malachite green (MG) from aqueous solutions. Contact time to reach equilibrium was reached after 300 min for both dyes and the PSO model predicted the best correspondence for the adsorption by almond shell. The authors further found that the film and pore diffusions are the rate-limiting steps in the adsorption onto this bio adsorbent.

Conclusions and future directions

The rate-limiting step (RLS) can play an important role in the uptake kinetic of dyes and is important for designing the adsorption system. Indeed, it is difficult to discuss the adsorption mechanism without the knowledge of RLS and where almost all kinetic studies have been directed towards the question of the rate-limiting step. The present work focused on the study of the limiting step which controls the sorption of organic matter in general and dyes in particular by different biomaterials such as algae, fungi, bacteria, agricultural, and industrial waste and plants.

Many kinetic models have been reported to study RLS in biosorption, such as pseudo first order, pseudo second order, Elovich, intraparticle diffusion, Bangham, external mass transfer, and Boyd. Generally, the pseudo second order (PSO) is capable of describing almost all kinetic data arising from the interactions of dyes with biomaterials. Thus, the dye adheres to the functional groups present on the surface of the biomaterial by chemical bonding where the adsorption rate depends on the absorption capacity and not on the initial concentration of the dye. The advantage of this model is that it allows the equilibrium adsorption capacity to be calculated. It is easy to understand that the adsorption of dyes onto biomaterials is complex and involves diffusions into both pores and films in the rate-limiting step.

Film diffusion takes place when external transfer is greater than internal transfer, while the opposite effect occurs in the case of porous diffusion which did not investigate the real rate-controlling step involved in the global adsorption, that is, the film or intraparticle diffusions. Until now, no kinetic model has proven generally suitable for determining the true flow limit step. However, the Boyd and intraparticle diffusion models are sufficient to analyze which is the true limiting step, filmic or intraparticle diffusion. Although RLS involved in dye adsorption has been studied for many years, the mechanism is not fully understood. So, our future direction to understand the adsorption mechanism is to discuss the rate-limiting stage where we will try to find a relationship between the thermodynamic parameters and the rate-limiting stage. Our perspective is to discuss the rate-limiting stage where we will try to find a relationship between the thermodynamic parameters and the rate-limiting stage.

Acknowledgements

The authors gratefully acknowledge support from the *Laboratory of Applied Chemistry and Materials (LabCAM), University of M'hamed Bougara of Boumerdes, Avenue de l'Indépendance Boumerdes, 35000. Algeria.* Laboratory of Coatings, Materials and Environment, University M'hamed Bougara (UMBB), Algeria. Laboratory of Storage and Valorization of Renewable Energies, Faculty of Chemistry (USTHB) Algeria. This research did not receive any specific grant from funding agencies in the public, commercial, or not-for-profit sectors.

Declaration of conflicting interests

The authors declared no potential conflicts of interest with respect to the research, authorship, and/or publication of this article.

Funding

The author(s) received no financial support for the research, authorship, and/or publication of this article.

Ethical statement

Ethical approval

Our study did not require an ethical board approval because it did not contain human or animal trials.

References

1. Liu W, Fan C, Zong Z, et al. Two Co(II)-Based metal organic frameworks for highly efficient removal of azo dyes from aqueous environment: synthesis, selective adsorption and adsorption mechanism. *Colloids Surf A Physicochem Eng Asp* 2020; 603: 125236.
2. Abbas M and Mohamed T. Contribution of adsorption and photocatalysis for the elimination of Black Eriochrome (NET) in an aqueous medium-Optimization of the parameters and Kinetics Modeling. *Scientific African* 2020; 8: 00387.
3. Abbas M. Contribution of Electrocoagulation Method in the removal of Fluorine ions from aqueous solution. *Desalination Water Treat* 2021; 226: 177–183.
4. Abbas M. Experimental investigation of Titanium Dioxide as an Adsorbent to remove Congo red from aqueous solution - equilibrium and Kinetics modeling. *Journal of Water and Reuse Desalination* 2020; 10(Issue 3): 251–266.
5. Abbas M. Performance of apricot stone (ACAS) to remove dyes from aqueous solutions –Equilibrium, Kinetics, Isotherms Modeling and Thermodynamic studies. *Mater Today Proc* 2020; 31: 437–443.
6. Arabkhani P and Asfaram A. Development of a novel three-dimensional magnetic polymer aerogel as an efficient adsorbent for malachite green removal, *J Hazard Mater* 2020; 384: 121394.
7. Abbas M and Mohamed T. Contribution of photocatalysis for the elimination of Methyl Orange (MO) in aqueous Medium using TiO_2 catalyst - optimization of the parameters and Kinetics modeling. *Desalination Water Treat* 2021; 214: 413–419.
8. Abbas M and Mohamed T. Photocatalytic degradation of asucryl red (GRL) in aqueous medium on heat-treated TiO_2 powder - effect of analytical parameters and kinetic modeling. *Desalination Water Treat* 2020; 180: 398–404.
9. Hassaan MA, El Nemr A and Madkour FF. Testing the advanced oxidation processes on the degradation of Direct Blue 86 dye in wastewater. *Egyptian Journal of Aquatic Research* 2017; 43: 11–19.
10. Abbas M. Photolyse of Bromophenol Blue in aquous solution under UV-irradiation: optimization of the parameters influencing the kinetics of degradation. *Desalination Water Treat* 2021; 216: 167–173.
11. Sahmoune MN, Louhab K and Boukhiar A. Advanced biosorbents materials for removal of chromium from water and wastewaters. *Environ Prog Sustain Energy* 2011; 30: 284–293.
12. Abbas M, Harrache Z and Mohamed T. Mass-transfer processes in the adsorption of crystal violet by activated carbon derived from pomegranate peels: kinetics and thermodynamic studies. *Journal of Engineered Fibers and Fabrics* 2020; 15: 1–11.
13. Abbas M. Experimental investigation of activated carbon prepared from apricot stones material (ASM) adsorbent for removal of malachite green (MG) from aqueous solution Adsorption. *Sci Technol* 2020; 38(1–2): 24–45.

14. Abbas M and Mohamed T. Removal of methylene blue (MB) in aqueous solution by economic adsorbent derived from apricot stone activated carbon (ASAC). *Fibers Polym* 2020; 21(No.4): 810–820.
15. Abbas M, Harrache Z and Mohamed T. Removal of Gentian Violet in aqueous solution by activated carbon equilibrium, kinetics, and thermodynamic study. *Adsorpt Sci Technol* 2019; 37(7–8): 566–589.
16. Harrache Z, Abbas M, Aksil T, et al. Thermodynamic and kinetics studies on adsorption of Indigo Carmine from aqueous solution by activated carbon. *Microchem J* 2019; 144: 180–189.
17. Pai S, Kini MS and Selvaraj R. A review on adsorptive removal of dyes from wastewater by hydroxyapatite nanocomposites. *Environ Sci Pollut Control Ser* 2021; 28: 11835–11849.
18. Katheresan V, Kansedo J and Lau SY. Efficiency of various recent wastewater dye removal methods: a review. *J Environ Chem Eng* 2018; 6: 4676–4697.
19. Yagub MT, Sen TK, Afroze S, et al. Dye and its removal from aqueous solution by adsorption: a review. *Adv Colloid Interface Sci* 2014; 209: 172–184.
20. Zhou Y, Lu J, Zhou Y, et al. Recent advances for dyes removal using novel adsorbents: a review. *Environ Pollut* 2019; 252: 352–365.
21. Kyzas GZ, N Bikiaris D and Cmitropoulos A. Chitosan adsorbents for dye removal: a review. *Polym Int* 2017; 66: 1800–1811.
22. Bhatia D, Sharma NR, Singh J, et al. Biological methods for textile dye removal from wastewater: a review. *Crit Rev Environ Sci Technol* 2017; 47: 1836–1876.
23. Marin P, Borba CE, Módenes AN, et al. Determination of the mass transfer limiting step of dye adsorption onto commercial adsorbent by using mathematical models. *Environ Technol* 2014; 35: 2356–2364.
24. Pauletto PS, Dotto GL and Salau NPG, Diffusion mechanisms and effect of adsorbent geometry on heavy metal adsorption, *Chem Eng Res Des* 2020; 157: 182–194.
25. da Rosa ALD, Carissimi E, Dotto GL, et al. Biosorption of rhodamine B dye from dyeing stones effluents using the green microalgae *Chlorella pyrenoidosa*. *J Clean Prod* 2018; 198: 1302–1310.
26. Sahmoune MN. *Épuration des eaux contaminées par des métaux lourds (chrome) à l'aide de résidus de fermentation fongique*. PhD thesis. Boumerdes, Algeria: University of Boumerdes, 2008.
27. Bharathi KS and Ramesh ST. Removal of dyes using agricultural waste as low-cost adsorbents: a review. *Appl Water Sci* 2013; 3: 773–790.
28. Nethaji S, Sivasamy A, Thennarasu G, et al. Adsorption of Malachite Green dye onto activated carbon derived from *Borassus aethiopum* flower biomass. *J Hazard Mater* 2010; 181: 271–280.
29. Viegas RMC, Campinas M, Costa H, et al. How do the HSDM and Boyd's model compare for estimating intraparticle diffusion coefficients in adsorption processes. *Adsorption* 2014; 20: 737–746.
30. Crini G, Lichtfouse E, Wilson L, et al. Adsorption-oriented processes using conventional and non-conventional adsorbents for wastewater treatment. *Green Adsorbents for Pollutant Removal, Springer Nature, Environmental Chemistry for a Sustainable World* 2018; 18: 23–71.
31. Wakkel M, Khiari B and Zagrouba F. Basic red 2 and methyl violet adsorption by date pits: adsorbent characterization, optimization by RSM and CCD, equilibrium and kinetic studies. *Environ Sci Pollut Control Ser* 2018; 26: 1–19.
32. Suzuki M. *Adsorption engineering*. Amsterdam: Kodansha LTD., Tokyo and Elsevier Science Publishers B. V., 1990.
33. Beekaroo D and Mudhoo A. Adsorption of reactive red 158 dye by chemically treated cocos nucifera L. Shell powder. *SpringerBriefs in Green Chemistry for Sustainability*. Berlin: Springer Dordrecht, 2011. DOI: 10.1007/978-94-007-1986-6.
34. Ouazene N and Sahmoune MN. Equilibrium and kinetic modelling of astrazon yellow adsorption by sawdust: effect of important parameters. *Int J Chem React Eng* 2010; 8: 151.

35. Sahmoune MN. Performance of *Streptomyces rimosus* biomass in biosorption of heavy metals from aqueous solutions. *Microchem J* 2018; 141: 87–95.
36. Sahmoune MN, Louhab K and Boukhiar A. Studies of chromium removal from tannery effluent by dead *Streptomyces rimosus*. *Chem Prod Process Model* 2008; 3: 29.
37. Mukherjee S and Halder G. A review on the sorptive elimination of fluoride from contaminated wastewater. *J Environ Chem Eng* 2018; 6: 1257–1270.
38. Sahmoune MN, Louhab K and Boukhiar A. Biosorption of Cr (III) from aqueous solutions using bacterium biomass *Streptomyces rimosus*. *Int J Environ Res* 2009; 3: 229–238.
39. Simonin J-P. On the comparison of pseudo-first order and pseudo-second order rate laws in the modeling of adsorption kinetics. *Chem Eng J (Lausanne)* 2016; 300: 254–263, DOI: 10.1016/j.cej.2016.04.079.
40. Sahmoune MN and Louhab K. Kinetic analysis of trivalent chromium biosorption by dead *Streptomyces rimosus* biomass. *Arabian J Sci Eng* 2010; 35: 69–80.
41. Sahmoune MN, Louhab K, Boukhiar A, et al. Kinetic and equilibrium models for the biosorption of Cr (III) on *Streptomyces rimosus*. *Toxicol Environ Chem* 2009; 91: 1291–1303.
42. Prajapati AK and Mondal MK. Comprehensive kinetic and mass transfer modeling for methylene blue dye adsorption onto CuO nanoparticles loaded on nanoporous activated carbon prepared from waste coconut shell. *J Mol Liq* 2020; 307: 112949.
43. Singh VP and Vaish R. Adsorption of dyes onto candle soot: equilibrium, kinetics and thermodynamics. *European Physical Journal Plus* 2018; 133: 446.
44. Ouznadji ZB, Sahmoune MN and Mezenner NY. Adsorptive removal of diazinon: kinetic and equilibrium study. *Desalination Water Treat* 2016; 57: 1880–1889.
45. Ahmad MA and Alrozi R. Removal of malachite green dye from aqueous solution using rambutan peel-based activated carbon: equilibrium, kinetic and thermodynamic studies. *Chem Eng J* 2011; 171: 510–516.
46. Spahn H and Schundler U. The scale-up of activate carbon columns for water purification, based on results from batch tests; theoretical and experimental determination of adsorption: rates of single organic solutes in batch testes. *Chem Eng Sci* 1975; 30: 529–537.
47. Sahmoune MN. The role of biosorbents in the removal of arsenic from water. *Chem Eng Technol* 2016; 39: 1617–1628.
48. Aravindhan R, Rao JR and Nair BU. Removal of basic yellow dye from aqueous solution by sorption on green alga *Caulerpa scalpelliformis*. *J Hazard Mater* 2007; 142: 68–76.
49. Khataee AR, Vafaei F and Jannatkhah M. Biosorption of three textile dyes from contaminated water by filamentous green algal Spirogyra sp.: kinetic, isotherm and thermodynamic studies. *Int Biodeterior Biodegrad* 2013; 83: 33–40.
50. El Atouani S, Belattmania Z, Reani A, et al. Brown seaweed *Sargassum muticum* as low-cost biosorbent of methylene blue. *Int J Environ Res* 2019; 13: 131–142.
51. Rubın E, Rodrıguez P, Herrero R, et al. Adsorption of methylene blue on chemically modified algal biomass: equilibrium, dynamic, and surface data. *J Chem Eng Data* 2010; 55: 5707–5714.
52. Daneshvar E, Kousha M, Sohrabi MS, et al. Biosorption of three acid dyes by the brown macroalga *Stoechospermum marginatum*: isotherm, kinetic and thermodynamic studies. *Chem Eng J* 2012; 195–196: 297–306.
53. Dotto GL and Pinto LAA. Analysis of mass transfer kinetics in the biosorption of synthetic dyes onto *Spirulina platensis* nanoparticles. *Biochem Eng J* 2012; 68: 85–90.
54. Krishna Prasad R and Srivastava SN. Sorption of distillery spent wash onto fly ash: kinetics and mass transfer studies. *Chem Eng J* 2009; 146: 90–97.

55. Vijayaraghavan K and Ashokkumar T. Characterization and evaluation of reactive dye adsorption onto biochar derived from *Turbinaria conoides* biomass. *Environ Prog Sustain Energy* 2019(4); 38: 13143. DOI: 10.1002/ep.13143.
56. Gupta VK, Bhushan R, Nayak A, et al. Biosorption and reuse potential of a blue green alga for the removal of hazardous reactive dyes from aqueous solutions. *Ann Finance* 2014; 18: 179–191.
57. Mullerova S, Baldikova E, Prochazkova J, et al. Magnetically modified macroalgae *Cymopolia barbata* biomass as an adsorbent for safranin O removal. *Mater Chem Phys* 2019; 225: 174–180.
58. Doğar C, Gurses A, Acıkyıldız M, et al. Thermodynamics and kinetic studies of biosorption of a basic dye from aqueous solution using green algae Ulothrix sp. *Colloids Surf B Biointerfaces* 2010; 76: 279–285.
59. Yu KL, Lee XJ, Ong HC, et al. Adsorptive removal of cationic methylene blue and anionic Congo red dyes using wet-torrefied microalgal biochar: equilibrium, kinetic and mechanism modeling. *Environ Pollut* 2021; 272: 115986.
60. Khambhaty Y, Mody K, Basha S, et al. Efficient removal of Brilliant Blue G (BBG) from aqueous solutions by marine Aspergillus wentii : kinetics, equilibrium and process design. *Ecol Eng* 2012; 41: 74–83.
61. Bayramoglu G and Arica MY. Adsorption of Congo Red dye by native amine and carboxyl modified biomass of *Funalia trogii*: isotherms, kinetics and thermodynamics mechanisms. *Kor J Chem Eng* 2018; 35: 1303–1311.
62. Bayramoglu G and Yilmaz M. Azo dye removal using free and immobilized fungal biomasses: isotherms, kinetics and thermodynamic studies. *Fibers Polym* 2018; 19: 877–886.
63. Chaudhry MT, Zohaib M, Rauf N, et al. Biosorption characteristics of *Aspergillus fumigatus* for the decolorization of triphenylmethane dye acid violet 49. *Appl Microbiol Biotechnol* 2014; 98: 3133–3141.
64. Salvi NA and Chattopadhyay S. Biosorption of Azo dyes by spent *Rhizopus arrhizus* biomass. *Appl Water Sci* 2017; 7: 3041–3054.
65. Bouras HD, Yeddou AR, Bouras N, et al. Biosorption of Congo red dye by *Aspergillus carbonarius* M333 and *Penicillium glabrum* Pg1: kinetics, equilibrium and thermodynamic studies. *J Taiwan Inst Chem Eng* 2017; 80: 915–923.
66. Pandey P, Singh RP, Singh KN, et al. Evaluation of the individuality of white rot macro fungus for the decolorization of synthetic dye. *Environ Sci Pollut Control Ser* 2013; 20: 238–249.
67. Dey MD, Shukla R, Bordoloi NK, et al. Mechanism of adsorptive removal of methylene blue using dried biomass of *Rhizopus oryzae*. *Appl Biochem Biotechnol* 2015; 177: 541–555.
68. Sintakindi A and Ankamwar B. Uptake of methylene blue from aqueous solution by naturally grown *Daedalea africana* and *Phellinus adamantinus* fungi. *ACS Omega* 2020; 5: 12905–12914.
69. Syafiuddin A and Fulazzaky MA. Decolorization kinetics and mass transfer mechanisms of Remazol Brilliant Blue R dye mediated by different fungi. *Biotechnology Reports* 2021; 29: e00573.
70. Saha PD, Bhattacharya P, Sinha K, et al. Biosorption of Congo red and Indigo carmine by nonviable biomass of a new Dietzia strain isolated from the effluent of a textile industry. *Desalination Water Treat* 2013; 51: 5840–5847.
71. Lin C, Gan L, Chen Z, et al. Biodegradation of Naphthalene using a functional biomaterial 3 based on immobilized *Bacillus fusiformis* (BFN). *Biochem Eng J* 2014; 90: 1–7.
72. Colak F, Atar N and Olgun A. Biosorption of acidic dyes from aqueous solution by *Paenibacillus macerans*: kinetic, thermodynamic and equilibrium studies. *Chem Eng J* 2009; 150: 122–130.
73. Yenikaya C, Atar E, Olgun A, et al. Biosorption study of anionic dyes from aqueous solutions using *Bacillus Amyloliquefaciens*. *Eng Life Sci* 2010; 10: 233–241.
74. Kim SY, Jin MR, Chung C, et al. Biosorption of cationic basic dye and cadmium by the novel biosorbent *Bacillus catenulatus* JB-022 strain. *J Biosci Bioeng* 2015; 119: 433–439.

75. Saravanan N, Kannadasan T, Basha CA, et al. Biosorption of textile dye using immobilized bacterial (*Pseudomonas aeruginosa*) and fungal (*Phanerochate chrysosporium*) cells. *Am J Environ Sci* 2013; 9: 377–387.
76. Zhou F, Cheng Y, Gan L, et al. *Burkholderia vietnamiensis* C09V as the functional biomaterial used to remove crystal violet and Cu(II). *EES (Ecotoxicol Environ Saf)* 2014; 105: 1–6.
77. Sahmoune MN. Evaluation of thermodynamic parameters for adsorption of heavy metals by green adsorbents. *Environ Chem Lett* 2019; 17: 697–704.
78. Binupriya AR, Sathishkumar M, Ku CS, et al. Sequestration of reactive blue 4 by free and immobilized *Bacillus subtilis* cells and its extracellular polysaccharides. *Colloids Surf B Biointerfaces* 2010; 76: 179–185.
79. Ashjaran A, Yazdanshenas ME, Rashidi A, et al. Biosorption thermodynamic and kinetic of direct dye from aqueous solutions on bacterial cellulose. *Afr J Microbiol Res* 2012; 6: 1270–1278.
80. Siddiqui SI, Rathi G and Chaudhry SA. Acid washed black cumin seed powder preparation for adsorption of methylene blue dye from aqueous solution: thermodynamic, kinetic and isotherm studies. *J Mol Liq* 2018; 264: 275–284.
81. Çelekli A, Al-Nuaimi AI and Bozkurt H. Adsorption kinetic and isotherms of reactive red 120 on *Moringa oleifera* seed as an eco-friendly process. *J Mol Struct* 2019; 1195: 168–178.
82. Wanyonyi WC, Onyari JM and Shiundu PM. Adsorption of Congo red dye from aqueous solutions using roots of *Eichhornia crassipes*: kinetic and equilibrium studies. *Energy Proc* 2014; 50: 862–869.
83. Jia Z, Li Z, Ni T, et al. Adsorption of low-cost absorption materials based on biomass (*Cortaderia selloana* flower spikes) for dye removal: kinetics, isotherms and thermodynamic studies. *J Mol Liq* 2017; 229: 285–292.
84. Oloo CM, Onyari JM, Wanyonyi WC, et al. Adsorptive removal of hazardous crystal violet dye form aqueous solution using *Rhizophora mucronata* stem-barks: equilibrium and kinetics studies. *Environmental Chemistry and Ecotoxicology* 2020; 2: 64–72.
85. Kooh MRR, Dahri MK, Lim LBL, et al. Batch adsorption studies on the removal of acid blue 25 from aqueous solution using *Azolla pinnata* and Soya bean waste. *Arabian J Sci Eng* 2016; 41: 2453–2464.
86. Carvalho LB, Chagas PMB and Pinto LMA, *Caesalpinia ferrea* fruits as a biosorbent for the removal of methylene blue dye from an aqueous medium, *Water, Air, & Soil Pollut* 2018; 229: 297–310.
87. Hassan W, Noureen S, Mustaqeem M, et al. Efficient adsorbent derived from *Haloxylon recurvum* plant for the adsorption of acid brown dye: kinetics, isotherm and thermodynamic optimization. *Surface Interfac* 2020; 20: 100510.
88. Wekoye JN, Wanyonyi WC, Wangila PT, et al. Kinetic and equilibrium studies of Congo red dye adsorption on cabbage waste powder. *Environmental Chemistry and Ecotoxicology* 2020; 2: 24–31.
89. Kumar M and Tamilarasan R. Kinetics and equilibrium studies on the removal of Victoria blue using Prosopis juliflora-modified carbon/Zn/alginate polymer composite beads. *J Chem Eng Data* 2013; 58: 517–527.
90. Hemmati F, Norouzbeigi R, Sarbisheh F, et al. Malachite green removal using modified sphagnum peat moss as a low-cost biosorbent: kinetic, equilibrium and thermodynamic studies. *J Taiwan Inst Chem Eng* 2016; 58: 482–489.
91. Kankılıç¸ GB, Metin AÜ and Tüzün I. *Phragmites australis*: an alternative biosorbent for basic dye removal. *Ecol Eng* 2016; 86: 85–94.
92. Chan SL, Tan YP, Abdullah A, et al. Equilibrium,kinetic and thermodynamic studies of a new potential biosorbent for the removal of Basic Blue3 and Congo Red dyes:Pineapple (*Ananascomosus*) plant stem. *J Taiwan Inst Chem Eng* 2016; 61: 306–315.
93. Ahmad R and Ansari K. Chemically treated *Lawsonia inermis* seeds powder (CTLISP): an eco-friendly adsorbent for the removal of brilliant green dye from aqueous solution. *Groundwater for Sustainable Development* 2020; 11: 100417.

94. Gupta VK, Pathania D, Agarwal S, et al. De-coloration of hazardous dye from water system using chemically modified Ficus carica adsorbent. *J Mol Liq* 2012; 174: 86–94.
95. Tran TH, Le AH, Pham TH, et al. Adsorption isotherms and kinetic modeling of methylene blue dye onto a carbonaceous hydrochar adsorbent derived from coffee husk waste. *Sci Total Environ* 2020; 725: 138325.
96. Karthika M and Vasuki M. Adsorption of Alizarine red-S dye from aqueous solution by Sago waste: resolution of isotherm, kinetics and thermodynamics. *Mater Today Proc* 2019; 14: 358–367.
97. Degermenci GD, Degermenci N, Ayvaoglu V, et al. Adsorption of reactive dyes on lignocellulosic waste; characterization, equilibrium, kinetic and thermodynamic studies. *J Clean Prod* 2019; 225: 1220–1229.
98. Sadaf S and Bhatti HN. Batch and fixed bed column studies for the removal of Indosol Yellow BG dye by peanut husk. *J Taiwan Inst Chem Eng* 2014; 45: 541–553.
99. Lim LBL, Priyantha N, Tennakoon DTB, et al. Breadnut peel as a highly effective low-cost biosorbent for methylene blue: equilibrium, thermodynamic and kinetic studies. *Arab J Chem* 2017; 10: S3216–S3228.
100. Soliman Nk, Moustafa AF, Aboud AA, et al. Effective utilization of Moringa seeds waste as a new green environmental adsorbent for removal of industrial toxic dyes. *J Mater Res Technol* 2019; 8: 1798–1808.
101. Stavrinou A, Aggelopoulos CA and Tsakiroglou CD. Exploring the adsorption mechanisms of cationic and anionic dyes onto agricultural waste peels of banana, cucumber and potato: adsorption kinetics and equilibrium isotherms as a tool. *J Environ Chem Eng* 2018; 6: 6958–6970.
102. Jiang Z and Hu D. Molecular mechanism of anionic dyes adsorption on cationized rice husk cellulose from agricultural wastes. *J Mol Liq* 2019; 276: 105–114.
103. Akar ST, Yilmazer D, Celik S, et al. On the utilization of a lignocellulosic waste as an excellent dye remover: modification, characterization and mechanism analysis. *Chem Eng J* 2013; 229: 257–266.
104. Nayak AK and Pal A. Rapid and high-performance adsorptive removal of hazardous acridine orange from aqueous environment using *Abelmoschus esculentus* seed powder: single- and multi-parameter optimization studies. *J Environ Manag* 2018; 217: 573–591.
105. Wakkel M, Khiari B and Zagrouba F. Textile wastewater treatment by agro-industrial waste: equilibrium modelling, thermodynamics and mass transfer mechanisms of cationic dyes adsorption onto low-cost lignocellulosic adsorbent. *J Taiwan Inst Chem Eng* 2019; 96: 439–452.
106. Sahmoune MN and Ouazene N. Mass-transfer processes in the adsorption of cationic dye by sawdust. *Environ Prog Sustain Energy* 2012; 31: 597–603.
107. Banerjee S and Chattopadhyaya MC. Adsorption characteristics for the removal of a toxic dye, tartrazine from aqueous solutions by a low cost agricultural by-product. *Arab J Chem* 2017; 10: S1629–S1638.
108. Ouazene N and Lounis A. Adsorption characteristics of CI basic blue 3 from aqueous solution onto Aleppo pine-tree sawdust. *Color Technol* 2011; 128: 21–27.
109. Inyinbor AA, Adekola FA and Olatunji GA. Kinetics, isotherms and thermodynamic modeling of liquid phase adsorption of RhodamineB dye onto *Raphia hookerie* fruit epicarp. *Water Resour Ind* 2016; 15: 14–27.
110. Dawood S and Sen TK. Removal of anionic dye Congo red from aqueous solution by raw pine and acid-treated pine cone powder as adsorbent: equilibrium, thermodynamic, kinetics, mechanism and process design. *Water Res* 2012; 46: 1933–1946.
111. Lima JP, Alvarenga G, Goszczynski ACF, et al. Batch adsorption of methylene blue dye using *Enterolobium contortisiliquum* as bioadsorbent: experimental, mathematical modeling and simulation. *J Ind Eng Chem* 2020; 91: 362–371.
112. Baidya KS and Kumar U. Adsorption of brilliant green dye from aqueous solution onto chemically modified areca nut husk. *South Afr J Chem Eng* 2021; 35: 33–43.
113. Ben Arfi R, Karoui S, Mougin K, et al. Adsorptive removal of cationic and anionic dyes from aqueous solution by utilizing almond shell as bioadsorbent. *Euro-Mediterranean Journal for Environmental Integration* 2017; 2: 20, DOI: 10.1007/s41207-017-0032-y.